



Measuring the frequency-time two-photon wavefunction of narrowband entangled photons from cold atoms via stimulated emission

KWANG-KYOON PARK,¹ JIN-HUN KIM,¹ TIAN-MING ZHAO,¹ YOUNG-WOOK CHO,² AND YOON-HO KIM^{1,*}

¹Department of Physics, Pohang University of Science and Technology (POSTECH), Pohang 37673, South Korea

²Center for Quantum Information, Korea Institute of Science and Technology, Seoul 02792, South Korea

*Corresponding author: yoonho72@gmail.com

Received 24 April 2017; revised 12 September 2017; accepted 16 September 2017 (Doc. ID 293457); published 12 October 2017

Cold atom based narrowband entangled photon sources are important for efficient atom–photon interaction, which is at the heart of long-distance quantum communication and quantum memory protocols. Complete characterization of the narrowband entangled photons requires acquiring the frequency-time two-photon wavefunction, involving both joint temporal intensity (JTI) and joint temporal phase (JTP) measurements. Here, we demonstrate stimulated emission tomography of the frequency-time two-photon wavefunction of narrowband entangled photons from cold atoms. We show more than six orders of magnitude ($\times 10^6$) improvement in the measurement time for obtaining JTI and JTP compared to the conventional direct photon counting method, thus paving the way toward ultrafast high-resolution quantum tomography of photonic quantum states. © 2017 Optical Society of America

OCIS codes: (270.0270) Quantum optics; (270.5585) Quantum information and processing; (190.4380) Nonlinear optics, four-wave mixing; (020.1670) Coherent optical effects.

<https://doi.org/10.1364/OPTICA.4.001293>

1. INTRODUCTION

Complete knowledge of a prepared quantum state is essential for quantum information processing, and it requires both amplitude and phase information of the quantum state. For discrete variable systems, such as N photonic polarization qubits, quantum state tomography allows us to reconstruct the N -qubit density matrix with 4^N projection measurements [1,2]. For continuous variable systems, the wavefunction of the system is of interest, and recent experiments have shown that measuring the transverse spatial wavefunction of a single photon is possible either by weak measurement [3,4] or by quantum interference [5]. Complete measurement of a multipartite wavefunction is thus of great interest and is essential for quantifying quantum correlation. However, even for much-studied photon pairs of spontaneous parametric downconversion, measuring both the joint amplitude and the joint phase of the state remains a challenging problem [6,7].

Among the variety of entangled two-photon sources, the cold atom based narrowband entangled photon source is of particular importance for efficient atom–photon interaction [8–12], which is at the heart of long-distance quantum communication and quantum memory protocols [13–15]. Recently, it has been reported that the cold atom based photon pair source can generate two photons entangled in a variety of degrees of freedom, such as frequency-time, position-momentum, polarization, orbital angular momentum, and hyper-entanglement [14,16–21]. Precise and fast measurement of the narrowband two-photon wavefunction,

therefore, is critical in experimental quantum information research. Complete characterization of the narrowband entangled photons is possible by acquiring the frequency-time two-photon wavefunction, involving both joint temporal intensity (JTI) and joint temporal phase (JTP) measurements. Note that the JTI of a narrowband two-photon state with a megahertz bandwidth can be directly measured with time-resolved two-photon detection by using commercially available single-photon-counting detectors [17]. The JTI measurement, however, requires a long accumulation time for the photon counting histogram, and the corresponding JTP measurement is nontrivial as it cannot be obtained by direct photon detection [22–24].

In this work, we propose and demonstrate a novel approach for measuring the frequency-time two-photon wavefunction of narrowband entangled photons from cold atoms via the classical stimulated four-wave mixing process. The JTI is obtained from the stimulated emission measurement by making use of the close connection between the spontaneous four-wave mixing (SFWM) process and its stimulated counterpart [25–30]. The JTP is obtained from interference between the seed beam and the corresponding stimulated emission beam. The JTI and JTP are measured in the same experimental setting, thus providing the complete frequency-time two-photon wavefunction of narrowband entangled photons. The two-photon wavefunction is then used to identify frequency-time entanglement between the two photons. Not only does our method allow us to obtain the

nontrivial JTP, but it also could offer more than six orders of magnitude ($\times 10^6$) improvement in the measurement time for obtaining JTI compared to the conventional direct photon counting method, thus paving the way toward ultrafast high-resolution quantum tomography of photonic quantum states.

2. EXPERIMENTAL SCHEMATIC AND THEORY

Let us first briefly describe the generation of frequency-time entangled narrowband photon pairs via SFWM in a cold atom cloud [9–12,17]. The Stokes (ω_s) and anti-Stokes (ω_{as}) photon pair is generated by the SFWM process at the 87 Rb magneto-optical trap (MOT) when the pump (ω_p) and coupling (ω_c) lasers are applied; see Fig. 1(a). The quantum state of the SFWM photon pair is given by

$$|\psi\rangle = \int dt_s dt_{as} \Psi(t_s, t_{as}) \hat{a}_s^\dagger(t_s) \hat{a}_{as}^\dagger(t_{as}) |0\rangle, \quad (1)$$

where $\hat{a}_s^\dagger(t_s)$ and $\hat{a}_{as}^\dagger(t_{as})$ are the creation operators for Stokes and anti-Stokes photons, respectively, $|0\rangle$ is the vacuum state, and $\Psi(t_s, t_{as})$ is the complex-valued two-photon wavefunction. The SFWM photon pair is then coupled into the single-mode fibers (SMFs) and directed to the temperature-stabilized solid etalon filters for blocking pump and coupling lasers.

The JTI, $|\Psi(t_s, t_{as})|^2$, can be acquired directly by time-resolved coincidence counting measurements with the condition that the inverse bandwidth of the photon pair should be much bigger than the time resolution of the detectors, i.e.,

$$\langle \psi | \hat{a}_s^\dagger(t_s) \hat{a}_{as}^\dagger(t_{as}) \hat{a}_{as}(t_{as}) \hat{a}_s(t_s) | \psi \rangle \propto |\Psi(t_s, t_{as})|^2. \quad (2)$$

As shown in Fig. 1(a), for the JTI measurement, the SFWM photons are detected with the single-photon detectors (SPDs), and the time-correlated single-photon-counting (TCSPC) module records the time-of-arrival histogram, which requires a long accumulation time [12,17]. The JTP measurement for the SFWM photons, however, is nontrivial as direct photon coincidence detection cannot reveal phase information. Quantum interferometric homodyne measurement, for instance, might provide JTP, but complete JTP measurement for a narrowband two-photon entangled state is a challenging problem [22,23]. Alternatively, one may utilize another degree of freedom, if available, for the JTP measurement. For instance, time-of-arrival histogram measurements at different polarization projection bases

could provide partial phase information of the state [24]. Obtaining the full JTP map in this way for an arbitrary two-photon entangled state, however, would not be feasible.

We now discuss how both JTI and JTP of the narrowband entangled photon pair from a cold atom cloud can be measured by using the stimulated four-wave mixing process. For the JTI measurement, the Stokes seed pulse is applied at the same time with the pump and the coupling lasers; see Fig. 1(b). The stimulated anti-Stokes pulse due to the Stokes seed pulse $|\alpha(t_s)\rangle$ is emitted backward at time t_{as} in the same direction as that of the spontaneously generated anti-Stokes photon, and its intensity can be described by

$$\langle \psi | D_s^\dagger[\alpha(t_s)] \hat{a}_s^\dagger(t_s) \hat{a}_{as}^\dagger(t_{as}) \hat{a}_{as}(t_{as}) \hat{a}_s(t_s) D_s[\alpha(t_s)] | \psi \rangle \propto |\alpha(t_s)|^2 |\Psi(t_s, t_{as})|^2, \quad (3)$$

where $D_s[\alpha(t_s)] \equiv \exp[\int dt_s \alpha(t_s) \hat{a}_s^\dagger(t_s) - \text{h.c.}]$ is the displacement operator and $|\alpha(t_s)|^2$ is the average photon number for the Stokes seed pulse. See Supplement 1 for further details [31]. The above result in Eq. (3) clearly shows that the JTI of the entangled photon pair in Eq. (2), which needs to be measured with time-resolved two-photon coincidence detection with two SPDs, can instead be acquired by measurement of the stimulated anti-Stokes pulse due to the stimulated four-wave mixing process. Moreover, since $|\alpha(t_s)|^2$ can be easily made to be large, the anti-Stokes pulse can be detected with a high-speed avalanche photodiode (APD), whose output is directly measured with a digital oscilloscope triggered by the Stokes seed pulse [26–29]. The stimulated emission approach to measuring JTI, therefore, promises orders of magnitude improvement in the measurement time.

For the JTP measurement, i.e., the phase measurement of the stimulated anti-Stokes pulse, the anti-Stokes cw seed β is applied additionally and interference between the anti-Stokes seed and the stimulated anti-Stokes pulse due to the Stokes seed is measured, resulting in the intensity variation ΔI of the anti-Stokes given as

$$\Delta I \propto |\Psi(t_s, t_{as}) \alpha(t_s) \beta| \cos[\phi(t_s, t_{as}) - \varphi_{\text{seed}}], \quad (4)$$

where φ_{seed} is the phase sum of the two seed beams with respect to the pump and coupling fields. See Supplement 1 for further details [31]. Thus, the JTP of the narrowband entangled photon pair, i.e., $\phi(t_s, t_{as}) = \arg[\Psi(t_s, t_{as})]$, can be extracted from the interference measurement.

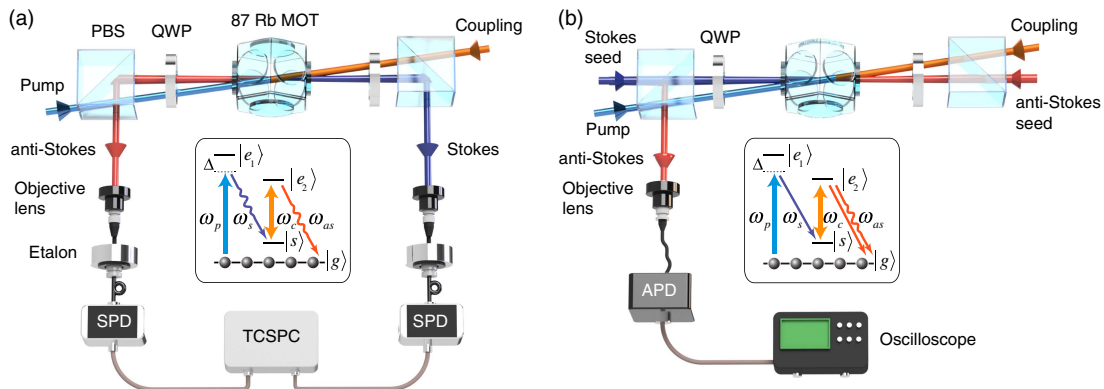


Fig. 1. Experimental setup. (a) JTI measurement scheme using time-resolved two-photon coincidence detection. (b) JTI and JTP measurement scheme with stimulated four-wave mixing. Note that unlike the spontaneous case, the etalon is unnecessary for blocking pumping lasers due to the high intensity of the stimulated field. PBS, polarizing beamsplitter; QWP, quarter wave plate.

3. COMPARISON OF THE SPONTANEOUS WITH THE STIMULATED

The essential features of the experiment are depicted in Fig. 1. A cold atomic ensemble of 87 Rb is prepared by a 2D MOT. After the initial loading, the MOT coil is turned off quickly to reduce the dephasing effect induced by the residual inhomogeneous magnetic fields. Then all the atoms are optically pumped into the ground state, $|g\rangle \equiv |5S_{1/2}, F=1\rangle$. The other relevant atomic levels are $|s\rangle \equiv |5S_{1/2}, F=2\rangle$, $|e_1\rangle \equiv |5P_{3/2}, F'=2\rangle$, and $|e_2\rangle \equiv |5P_{1/2}, F'=2\rangle$. The pump detuning is $\Delta = 62.9$ MHz. We characterize the medium properties such as optical depth (OD) and ground state dephasing rate γ_{gs} by measuring the electromagnetically induced transparency (EIT) transmission spectrum [32,33].

The frequency-time entangled narrowband Stokes and anti-Stokes photon pair can be generated via SFWM when pump and coupling lasers are applied to the cold atom medium as shown in Fig. 1(a) [9–12,17]. The cold atomic ensemble facilitates the generation of the narrowband photon pairs via $\chi^{(3)}$ nonlinearity of the medium enhanced by EIT [11]. The pump power and the coupling power, respectively, are roughly 100 μ W and 1 mW. Both the pump and the coupling lasers are well collimated to illuminate the whole ensemble (~ 2.1 mm in diameter). The SFWM photon pair is collected at 0.3° from the line of the pump and coupling lasers. A solid etalon with a full width at half maximum (FWHM) bandwidth of 470 MHz is used in each path to filter out the scattered light from the pump and coupling lasers. The SFWM photon pair is finally detected with the SPDs, and the TCSPC module records the time-of-arrival histogram [12,17]. For measuring JTI and JTP via stimulated four-wave mixing, we apply Stokes and anti-Stokes seed lasers to the cold atom cloud, and the diameter of the Stokes and anti-Stokes fields is roughly 500 μ m at the medium. The applied laser fields, SFWM photons, and stimulated emission are all circularly polarized in the frame of the atom.

We first compare the time-resolved two-photon waveform of SFWM and the anti-Stokes output of stimulated four-wave mixing. The time-resolved two-photon waveform measurement of the SFWM photon pair as shown in Fig. 2(a) is performed by using the experimental setup shown in Fig. 1(a). Here, the experiment is repeated every 50 ms: the SPDs are turned on for 1 ms for photon counting, and the rest of the time is used for loading Rb atoms into the MOT. The effective accumulation time of the coincidence counts excluding the medium preparation period is 60 s. The anti-Stokes output due to stimulated four-wave mixing is measured with the experimental setup shown in Fig. 1(b). Figure 2(b) shows the anti-Stokes intensity measured with the APD after the 20 ns Stokes seed pulse is applied at t_s . The data represent the averaged intensity of 20 oscilloscope traces during the 34 μ s accumulation time. The stimulated emission method not only shows the corresponding two-photon waveform with a high signal-to-noise ratio, but also offers more than six orders of magnitude ($\times 10^6$) improvement in the measurement time for obtaining the two-photon waveform compared to the direct photon counting approach.

4. COMPLETE MEASUREMENT OF THE TWO-PHOTON WAVEFUNCTIONS

Frequency-time entanglement between the narrowband SFWM photon pair can be engineered by properly choosing the pump

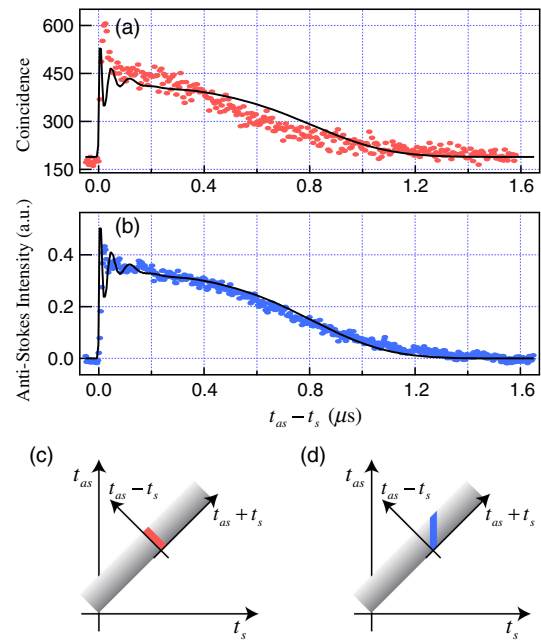


Fig. 2. Two-photon waveform measurement. (a) Time-resolved two-photon detection. The red dots represent the coincidence counts accumulated for 60 s (excluding the MOT preparation time). (b) Stimulated four-wave mixing. The intensity of anti-Stokes emission is measured when the Stokes seed pulse of 20 ns is applied at t_s . The blue dots represent the averaged intensity of 20 oscilloscope traces during the 34 μ s accumulation time. The black solid line in (a) and (b) is the theoretical curve for the two-photon waveform calculated with the experimental parameters OD = 53, $\gamma_{gs}/2\pi = 16.8$ kHz, and $\Omega_c/2\pi = 7.2$ MHz. Note that, since the TCSPC measures the coincidence histogram in the $t_{as} - t_s$ axis via the start–stop measurement, the two-photon measurement data in (a) correspond to the red cross section of the JTI shown in (c). For the stimulated emission, the anti-Stokes pulse is measured at a specific Stokes pulse time t_s , corresponding to the blue cross section shown in (d), which is not corresponding to the $t_{as} - t_s$ axis. For the same comparison, the time axis in (b) thus has been scaled by $1/\sqrt{2}$ to project onto the $t_{as} - t_s$ axis.

pulsewidth, the Rabi frequency of the coupling field, the OD of the medium, etc., to generate time-correlated (frequency-anticorrelated), time-uncorrelated (frequency-uncorrelated), or time-anticorrelated (frequency-correlated) photon pairs [17]. In this experiment, by using stimulated four-wave mixing in a cold atom cloud, we fully measure the frequency-time two-photon wavefunction (i.e., JTI and JTP) of narrowband entangled photons for the two cases that are important: time-correlated and time-uncorrelated narrowband SFWM photon pairs.

The experimental data for the time-correlated two-photon wavefunction of narrowband entangled photons is shown in Fig. 3. The pump pulsewidth in this case is 1 μ s. For the JTI measurement via stimulated four-wave mixing, it is necessary to apply a proper Stokes seed pulse to resolve the 400 ns two-photon coherence time of the photon pair. In this experiment, the Stokes seed pulsewidth is set at 20 ns, which is sufficient to resolve the whole JTI map with the resolution of 20 ns. With the Stokes seed pulse applied at time t_s along with the pump pulse and coupling, the stimulated anti-Stokes pulse is emitted and its temporal shape in time t_{as} corresponds to a column section of the JTI at time t_s . By varying t_s , we obtain the JTI measurement shown in

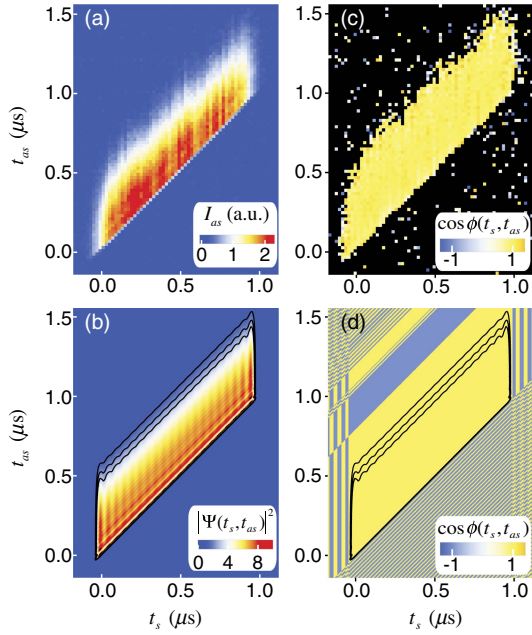


Fig. 3. Frequency-time two-photon wavefunction for time-correlated narrowband photon pair. (a) Experimental JTI measured via stimulated four-wave mixing. The color bar represents the intensity of the stimulated anti-Stokes pulse. (b) Theoretical JTI. The unit of the color bar is $10^{-5} \mu\text{s}^{-2}$. (c) Corresponding experimental JTP from interference. The color bar corresponds to the cosine of JTP. The black areas represent phase undefined regions due to vanishing JTI. (d) Theoretical JTP. The black contour lines in (c) and (d) represent the isoheight JTI lines.

Fig. 3(a). The JTI measurement via stimulated four-wave mixing in Fig. 3(a) agrees well with the theoretical JTI shown in Fig. 3(b). The theoretical JTI is numerically calculated by integrating the two-photon wavefunction in Eq. (2), which includes the $\chi^{(3)}$ non-linearity of the cold atom medium, the phase matching function, and the pump function [17]. The pump function is assumed to be rectangular in time, and the parameters for numerical calculation are set with the measured experimental parameters of $\text{OD} = 53$, $\gamma_{\text{gs}}/2\pi = 16.8$ kHz, and the coupling Rabi frequency $\Omega_c/2\pi = 10.0$ MHz.

Let us now consider the JTP measurement via stimulated four-wave mixing. In order to obtain JTP of the frequency-time entangled narrowband photon pair via stimulated emission, we make use of the interference effect described in Eq. (4) by additionally applying the anti-Stokes seed pulse as shown in Fig. 1(b). From the interference measurement data and $|\Psi(t_s, t_{as})|$ obtained from JTI, it is possible to extract JTP, i.e., $\cos \phi(t_s, t_{as})$, by using Eq. (4). The JTP measurement is shown in Fig. 3(c). It is clear from the data that the phase is constant with $\cos \phi(t_s, t_{as}) = 1$ over the entire nonzero JTI region. The JTP data show good agreement with the theoretical JTP shown in Fig. 3(d). Note that we could measure the JTP without phase-locking between the pumps and the seeds as the single-shot measurement was enough for acquiring meaningful data.

The experimental data for the time-uncorrelated two-photon wavefunction of narrowband entangled photons is shown in Fig. 4. The pump pulsewidth in this case is 200 ns. As before, the JTI measurement via stimulated four-wave mixing in Fig. 4(a) agrees well with the theoretical JTI in Fig. 4(b). In

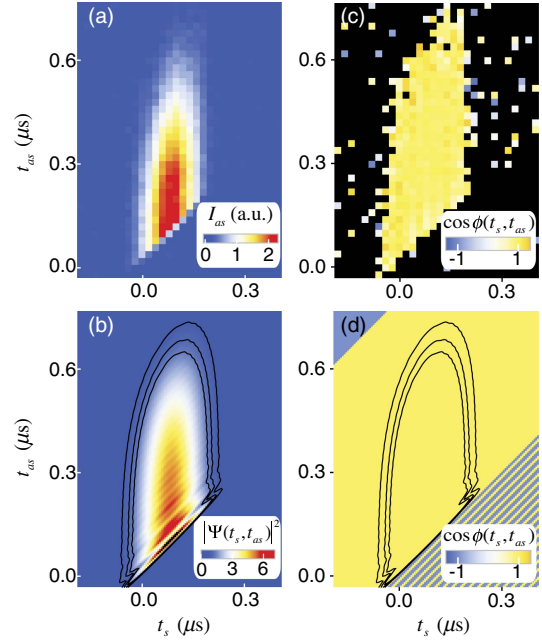


Fig. 4. Frequency-time two-photon wavefunction for time-uncorrelated narrowband photon pair. (a) Experimental JTI measured via stimulated four-wave mixing. The color bar represents the intensity of the stimulated anti-Stokes pulse. (b) Theoretical JTI. The unit of the color bar is $10^{-4} \mu\text{s}^{-2}$. (c) Corresponding experimental JTP from interference. The color bar corresponds to the cosine of JTP. The black areas represent phase undefined regions due to vanishing JTI. (d) Theoretical JTP. The black contour lines in (c) and (d) represent the isoheight JTI lines.

calculating the theoretical JTI in Fig. 4(b), we have assumed that the pump function has the Gaussian shape of 200 ns in time, and the same cold atom parameters as before are used.

The JTI and JTP data set, measured via stimulated four-wave mixing, together constitutes the frequency-time two-photon wavefunction of the narrowband entangled photon pair, and therefore it can be used to quantify frequency-time entanglement of the photon pair. To quantify the amount of entanglement, we apply Schmidt analysis to the JTI/JTP data set, which is already discretized in the form of a matrix [34,35]. The entropy of entanglement S and the purity of the heralded single photon P are obtained from the eigenvalues λ_i of the joint temporal wavefunction matrix, where $S \equiv -\sum_i \lambda_i \log_2 \lambda_i$ and $P \equiv \sum_i \lambda_i^2$. For the time-correlated photon pair represented in Figs. 3(a) and 3(c), we experimentally obtain $S_L = 2.44$ and $P_L = 0.294$, which are consistent with the theoretical values of $S_L = 2.12$ and $P_L = 0.345$ obtained from Figs. 3(b) and 3(d). For the time-uncorrelated photon pair depicted in Figs. 4(a) and 4(c), we experimentally obtain $S_S = 0.958$ and $P_S = 0.741$. The theoretical values evaluated from Figs. 4(b) and 4(d) are $S_S = 0.679$ and $P_S = 0.822$.

5. CONCLUSION

In summary, we have demonstrated a novel approach for measuring the frequency-time two-photon wavefunction of narrowband entangled photons from cold atoms via stimulated emission. By measuring JTI and JTP of a two-photon quantum state via the classical stimulated four-wave mixing process and

interference, we demonstrate that the quantum two-photon wavefunction may be efficiently obtained from classical signals. We have shown that our method could offer more than six orders of magnitude ($\times 10^6$) improvement in the measurement time for obtaining JTI and JTP compared to the conventional direct photon counting method, thus paving the way toward ultrafast high-resolution quantum tomography of photonic quantum states.

Funding. Samsung Science & Technology Foundation (SSTF-BA1402-07).

See [Supplement 1](#) for supporting content.

REFERENCES AND NOTES

1. A. G. White, D. James, P. H. Eberhard, and P. G. Kwiat, "Nonmaximally entangled states: production, characterization, and utilization," *Phys. Rev. Lett.* **83**, 3103–3107 (1999).
2. D. F. V. James, P. G. Kwiat, W. J. Munro, and A. G. White, "Measurement of qubits," *Phys. Rev. A* **64**, 052312 (2001).
3. J. S. Lundeen, B. Sutherland, A. Patel, C. Stewart, and C. Bamber, "Direct measurement of the quantum wavefunction," *Nature* **474**, 188–191 (2011).
4. M. Mirhosseini, O. S. Magaña-Loaiza, S. M. H. Rafsanjani, and R. W. Boyd, "Compressive direct measurement of the quantum wave function," *Phys. Rev. Lett.* **113**, 090402 (2014).
5. R. Chrapkiewicz, M. Jachura, K. Banaszek, and W. Wasilewski, "Hologram of a single photon," *Nat. Photonics* **10**, 576–579 (2016).
6. W. Wasilewski, P. Wasylczyk, P. Kolenderski, K. Banaszek, and C. Radzewicz, "Joint spectrum of photon pairs measured by coincidence Fourier spectroscopy," *Opt. Lett.* **31**, 1130–1132 (2006).
7. W. Wasilewski, P. Kolenderski, and R. Frankowski, "Spectral density matrix of a single photon measured," *Phys. Rev. Lett.* **99**, 123601 (2007).
8. A. Kuzmich, W. P. Bowen, A. D. Boozer, A. Boca, C. W. Chou, L.-M. Duan, and H. J. Kimble, "Generation of nonclassical photon pairs for scalable quantum communication with atomic ensembles," *Nature* **423**, 731–734 (2003).
9. V. Balić, D. A. Braje, P. Kolchin, G. Y. Yin, and S. E. Harris, "Generation of paired photons with controllable waveforms," *Phys. Rev. Lett.* **94**, 183601 (2005).
10. S. Du, P. Kolchin, C. Belthangady, G. Y. Yin, and S. E. Harris, "Subnatural linewidth biphotons with controllable temporal length," *Phys. Rev. Lett.* **100**, 183603 (2008).
11. S. Du, J. Wen, and M. H. Rubin, "Narrowband biphoton generation near atomic resonance," *J. Opt. Soc. Am. B* **25**, C98–C108 (2008).
12. Y.-W. Cho, K.-K. Park, J.-C. Lee, and Y.-H. Kim, "Generation of nonclassical narrowband photon pairs from a cold rubidium cloud," *J. Korean Phys. Soc.* **63**, 943–950 (2013).
13. X.-H. Bao, X.-F. Xu, C.-M. Li, Z.-S. Yuan, C.-Y. Lu, and J.-W. Pan, "Quantum teleportation between remote atomic-ensemble quantum memories," *Proc. Natl. Acad. Sci. USA* **109**, 20347–20351 (2012).
14. D.-S. Ding, W. Zhang, Z.-Y. Zhou, S. Shi, B.-S. Shi, and G.-C. Guo, "Raman quantum memory of photonic polarized entanglement," *Nat. Photonics* **9**, 332–338 (2015).
15. S.-J. Yang, X.-J. Wang, X.-H. Bao, and J.-W. Pan, "An efficient quantum light-matter interface with sub-second lifetime," *Nat. Photonics* **10**, 381–384 (2016).
16. H. Yan, S. Zhang, J. F. Chen, M. M. T. Loy, G. K. L. Wong, and S. Du, "Generation of narrow-band hyperentangled nondegenerate paired photons," *Phys. Rev. Lett.* **106**, 033601 (2011).
17. Y.-W. Cho, K.-K. Park, J.-C. Lee, and Y.-H. Kim, "Engineering frequency-time quantum correlation of narrow-band biphotons from cold atoms," *Phys. Rev. Lett.* **113**, 063602 (2014).
18. K. Liao, H. Yan, J. He, S. Du, Z.-M. Zhang, and S.-L. Zhu, "Subnatural-linewidth polarization-entangled photon pairs with controllable temporal length," *Phys. Rev. Lett.* **112**, 243602 (2014).
19. D.-S. Ding, W. Zhang, Z.-Y. Zhou, S. Shi, G.-Y. Xiang, X.-S. Wang, Y.-K. Jiang, B.-S. Shi, and G.-C. Guo, "Quantum storage of orbital angular momentum entanglement in an atomic ensemble," *Phys. Rev. Lett.* **114**, 050502 (2015).
20. J.-C. Lee, K.-K. Park, T.-M. Zhao, and Y.-H. Kim, "Einstein-Podolsky-Rosen entanglement of narrowband photons from cold atoms," *Phys. Rev. Lett.* **117**, 250501 (2016).
21. W. Zhang, D.-S. Ding, M.-X. Dong, S. Shi, K. Wang, S.-L. Liu, Y. Li, Z.-Y. Zhou, B.-S. Shi, and G.-C. Guo, "Experimental realization of entanglement in multiple degrees of freedom between two quantum memories," *Nat. Commun.* **7**, 13514 (2016).
22. F. A. Beduini, J. A. Zielińska, V. G. Lucivero, Y. A. de Icaza Astiz, and M. W. Mitchell, "Interferometric measurement of the biphoton wave function," *Phys. Rev. Lett.* **113**, 183602 (2014).
23. C. Ren and H. F. Hofmann, "Analysis of the time-energy entanglement of down-converted photon pairs by correlated single-photon interference," *Phys. Rev. A* **86**, 043823 (2012).
24. P. Chen, C. Shu, X. Guo, M. M. T. Loy, and S. Du, "Measuring the biphoton temporal wave function with polarization-dependent and time-resolved two-photon interference," *Phys. Rev. Lett.* **114**, 010401 (2015).
25. M. Liscidini and J. E. Sipe, "Stimulated emission tomography," *Phys. Rev. Lett.* **111**, 193602 (2013).
26. B. Fang, O. Cohen, M. Liscidini, J. E. Sipe, and V. O. Lorenz, "Fast and highly resolved capture of the joint spectral density of photon pairs," *Optica* **1**, 281–284 (2014).
27. A. Eckstein, G. Boucher, A. Lemaître, P. Filloux, I. Favero, G. Leo, J. E. Sipe, M. Liscidini, and S. Ducci, "High-resolution spectral characterization of two photon states via classical measurements," *Laser Photon. Rev.* **8**, L76–L80 (2014).
28. M. Avenhaus, B. Brecht, K. Laiho, and C. Silberhorn, "Time-frequency quantum process tomography of parametric down-conversion," *arXiv:1406.4252* (2014).
29. L. A. Rozema, C. Wang, D. H. Mahler, A. Hayat, A. M. Steinberg, J. E. Sipe, and M. Liscidini, "Characterizing an entangled-photon source with classical detectors and measurements," *Optica* **2**, 430–433 (2015).
30. I. Jizan, B. Bell, L. G. Helt, A. C. Bedoya, C. Xiong, and B. J. Eggleton, "Phase-sensitive tomography of the joint spectral amplitude of photon pair sources," *Opt. Lett.* **41**, 4803–4806 (2016).
31. See [Supplement 1](#) for the details of the derivation.
32. M. Fleischhauer and M. Lukin, "Dark-state polaritons in electromagnetically induced transparency," *Phys. Rev. Lett.* **84**, 5094–5097 (2000).
33. M. Fleischhauer, A. Imamoglu, and J. P. Marangos, "Electromagnetically induced transparency: optics in coherent media," *Rev. Mod. Phys.* **77**, 633–673 (2005).
34. C. K. Law, I. A. Walmsley, and J. H. Eberly, "Continuous frequency entanglement: effective finite Hilbert space and entropy control," *Phys. Rev. Lett.* **84**, 5304–5307 (2000).
35. P. J. Mosley, J. S. Lundeen, B. J. Smith, and I. A. Walmsley, "Conditional preparation of single photons using parametric downconversion: a recipe for purity," *New J. Phys.* **10**, 093011 (2008).